The study of participant-spectator matter and collision dynamics in heavy-ion collisions

Aman D. Sood and Rajeev K. Puri
Department of Physics, Panjab University, Chandigarh -160 014, India.

April 6, 2010

Abstract

We present the simulations of heavy-ion collisions in terms of participant-spectator matter. We find that this matter depends crucially on the collision dynamics and history of the nucleons. The important changes in the momentum space are due to the binary nucleon-nucleon collisions experienced during the high dense phase. This was otherwise not possible with mean field alone. The collisions push the colliding nucleons into midrapidity region responsible for the formation of participant matter. This ultimately leads to thermalization in heavy-ion collisions.

Electronic address: rkpuri@pu.ac.in

1 Introduction

The heavy-ion collisions at intermediate energies are the center of present day nuclear research. This is because of several rare phenomena emerging at these energies and also their utility in several other branches of physics.[1, 2, 3] The study of hot and dense matter and its relation to nuclear equation of state and cross section has always fascinated the researchers.[1, 2, 3, 4, 5, 6] Some of the rare phenomena emerging are the multifragmentation,[1, 2, 3] collective flow,[2, 3] stopping[2, 3] as well as subthreshold particle production[7] etc. In the low energy heavy-ion collisions, the fusion and decay of excited compound nucleus and fission dominate the physics.[8] Whereas at high incident energies, the transparency and complete disassembly of nuclear matter happens. In terms of theoretical description, the relative dominance of real and imaginary parts of G-matrix decides the fate of a reaction.[9] At low incident energies, the Pauli principle forbids the nucleon-nucleon binary collisions and scattering.[1, 2, 3] The attractive mean field decides the fate of colliding pairs. This results into fusion and consequently, into its decay. The frequent nucleon-nucleon collisions at high incident energies make imaginary part very significant. However, both real and imaginary parts of complex G-matrix are equally important at intermediate energies. This picture can also be looked in terms of participant-spectator matter and fireball concept.[1, 10] The nucleon-nucleon collisions play an important role in destroying the mutual initial nucleon-nucleon correlations and memory of nucleons. This ultimately leads to the above rare phenomena at intermediate energies.

We here plan to understand the formation of participant-spectator matter and its development in terms of collision dynamics. Recently, participant-spectator matter has been found to be independent of the system size at energy of vanishing flow. Therefore, it acts as a barometer for the study of disappearance of flow and balance energy.[10, 11] Section 2, describes the model briefly. In section 3, we present our results and section 4 summarizes the outcome.

2 The model

We simulate the nucleons within the framework of quantum molecular dynamics (QMD) model. In the QMD model,[2, 3] each nucleon propagates under the influence of mutual interactions. The propagation is governed by

the classical equations of motion:

$$\dot{\mathbf{r}}_i \;=\; \frac{\partial H}{\partial \mathbf{p}_i};\; \dot{\mathbf{p}}_i \;=\; -\frac{\partial H}{\partial \mathbf{r}_i}, \tag{1}$$

where H stands for the Hamiltonian which is given by:

$$H = \sum_i^A \frac{\mathbf{p}_i^2}{2m_i} + \sum_i^A (V_i^{Skyrme} + V_i^{Yuk} + V_i^{Coul}). \tag{2}$$

The V_i^{Skyrme}, V_i^{Yuk}, and V_i^{Coul} in Eq. (2) are, respectively, the Skyrme, Yukawa, and Coulomb potentials.

3 Results and Discussion

We here simulated the reactions of ^{40}Ca+^{40}Ca and ^{131}Xe+^{131}Xe, at different colliding geometries. This varies from very central ($b = 0$ fm) to peripheral one ($b = R_1 + R_2$; R_i is the radius of either target or projectile). The incident energy is also varied between 200 and 400 MeV/nucleon. In the present study, we use a hard equation of state along with nucleon-nucleon cross section $\sigma = 40$ mb. As discussed by many authors, the dynamics is insensitive towards the nuclear equation of state as well as towards nucleon-nucleon cross section. However, the above equation of state and cross section has been reported to reproduce the balance energy over wide range of colliding masses.[11]

The present participant-spectator matter demonstration is based on the definition reported in our earlier recent publication.[11] Here participant-spectator matter is defined in two different ways. (a) In the first definition, all nucleons experiencing at least one collision are labeled as participant matter. The remaining nucleons are the part of spectator matter. (b) In the second definition, the above demarcation is based on the experimental method, where one uses different rapidity cuts to define participant and spectator matter. The rapidity of ith particle is defined as

$$Y(i) = \frac{1}{2} \ln \frac{\mathbf{E}(i) + \mathbf{p}_z(i)}{\mathbf{E}(i) - \mathbf{p}_z(i)}, \tag{3}$$

where $\mathbf{E}(i)$ and $\mathbf{p}_z(i)$ are, respectively, the total energy and longitudinal momentum of ith particle. Now one can impose different cuts to study the

different participant-spectator matter. We shall here use the first definition to construct the participant-spectator matter. However, one should note that both these definitions have been reported to give same results.[10]

In Figs. 1 and 2, we display the time evolution, respectively, in the spatial and momentum spaces for the central collision of ^{40}Ca+^{40}Ca at 200 MeV/nucleon. The solid (open) circles denote the spectator (participant) matter. During initial stages of the reaction (till 10 fm/c), projectile and target are well separated both in the coordinate and momentum spaces. As a result, whole of the matter is in the form of spectator matter only. As the nuclei overlap, the density increases, that leads to more and more nucleon-nucleon binary collisions. This changes the matter from spectator to participant one. Due to the frequent nucleon-nucleon collisions, nucleons scatter in the transverse direction also. With the evolution of the reaction, participant matter increases, leading to more nucleons scattering in the transverse direction. At the end of the reaction, we see only a few spectator nucleons.

Looking at the momentum space (Fig. 2), we see that the spectator nucleons have very little change in their initial velocity profile over the period of the reaction. On the other hand, participant matter leads the matter into midrapidity region. This drives the system into global equilibrium. Naturally, more the initial correlations are destroyed, more is the system close to the global equilibrium. Since, these figures are the snapshots of a single event, the picture could be different for different events. The matter is cold and fragmented at the final state. This may lead to the idea that compressed matter expands and due to Coulomb instabilities, this breaks into pieces. However, this argument has been questioned by one of us and collaborators who were able to detect the fragments at the time when matter is compressed and hot.[12] If one evolutes the reaction between time steps 10-30 fm/c, one sees that the density rises from 0.9 to 1.7 between 10-20 fm/c, and falls by the same amount between 20-30 fm/c. However, the average collision number is not symmetric. The collision rate between 20-30 fm/c is higher than between 10-20 fm/c. This points toward the compactness of the nucleons in space with slower velocities.

In Figs. 3 and 4, we display the same evolution, but at colliding geometries of $b/b_{max} = 0.2$, 0.65, and 0.95, respectively. The solid (open) symbols represent spectator (participant) matter. The left panels of the figures are for the participant-spectator matter formed at the time of high density. The right panels are for the participant-spectator matter emerging at diluted phase of the density. Note that at this state, the matter is cold and

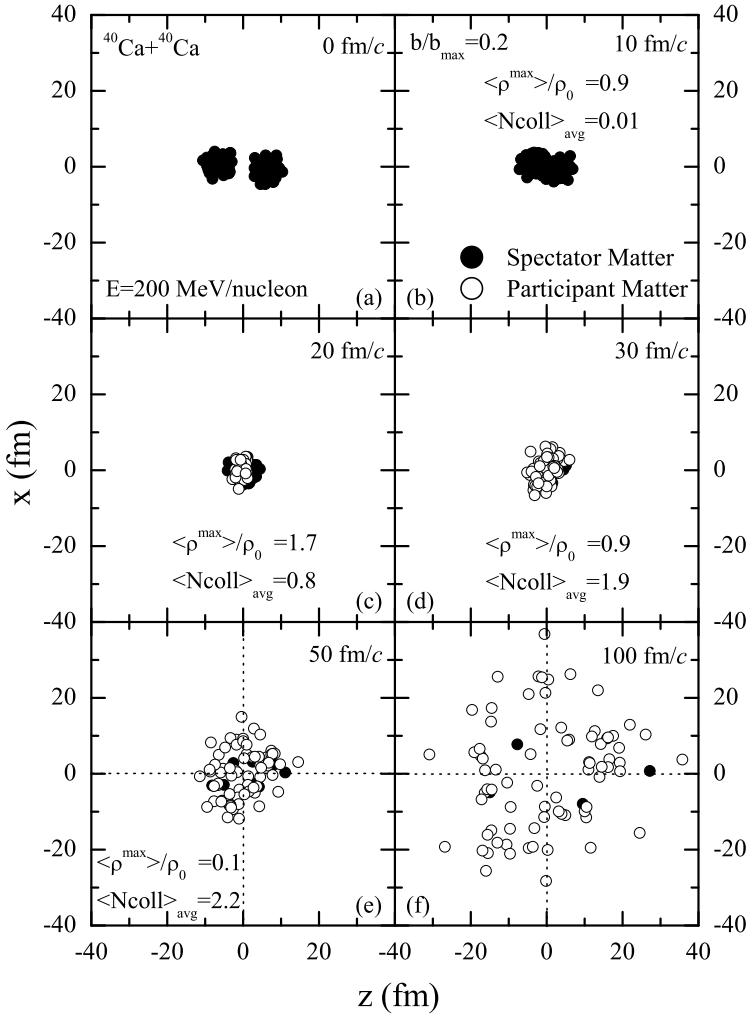

Figure 1: The time evolution of a single event of ^{40}Ca+^{40}Ca reaction at 200 MeV/nucleon and $b/b_{max} = 0.2$ in coordinate space. The solid (open) circles represent spectator (participant) matter, respectively. The $< \rho^{max} > /\rho_0$ and $< Ncoll >_{avg}$ are the maximum density and average number of nucleon-nucleon collisions averaged over large number of events.

fragmented. The reaction time for the high densities is around 20 fm/c for $b/b_{max} = 0.2$, 0.65, and 0.95 as is also evident from Fig. 1. Note that the time of maximal density varies linearly with the size of interacting nuclei.[5, 10]

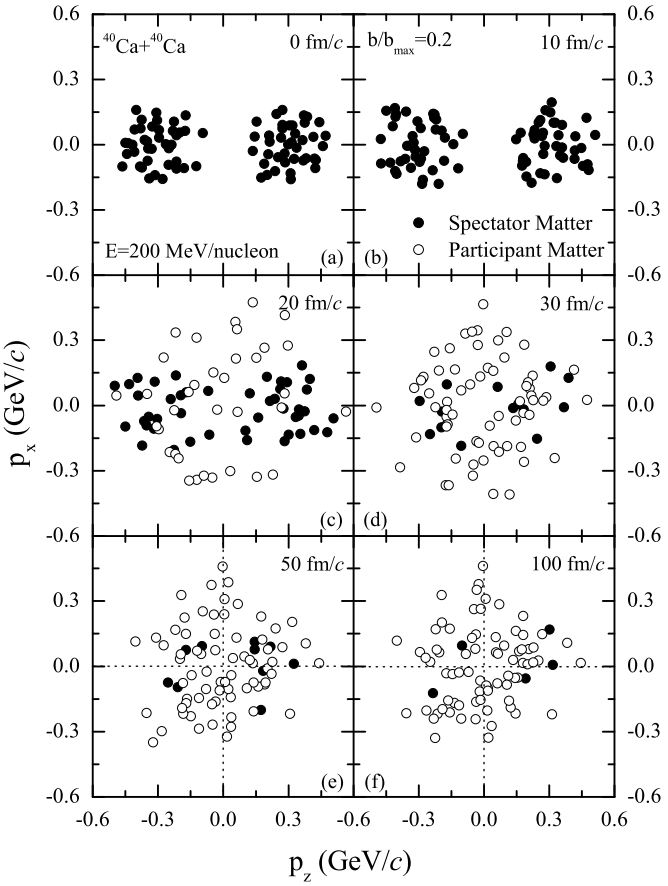

Figure 2: Same as Fig. 1, but in momentum space.

From the figures, one notices a reduced intensity of the participant matter with increase in the impact parameter. At central impact parameters, nucleons are well scattered in the momentum space. However, one can see two well separated momentum spaces at higher impact parameters. This indicates that momentum correlations remain preserved till the end of the reaction. Further, central collisions lead to significant portion as participant matter at high density. On the other hand, it is almost spectator matter at peripheral geometries. One may say that the reaction in central collisions is

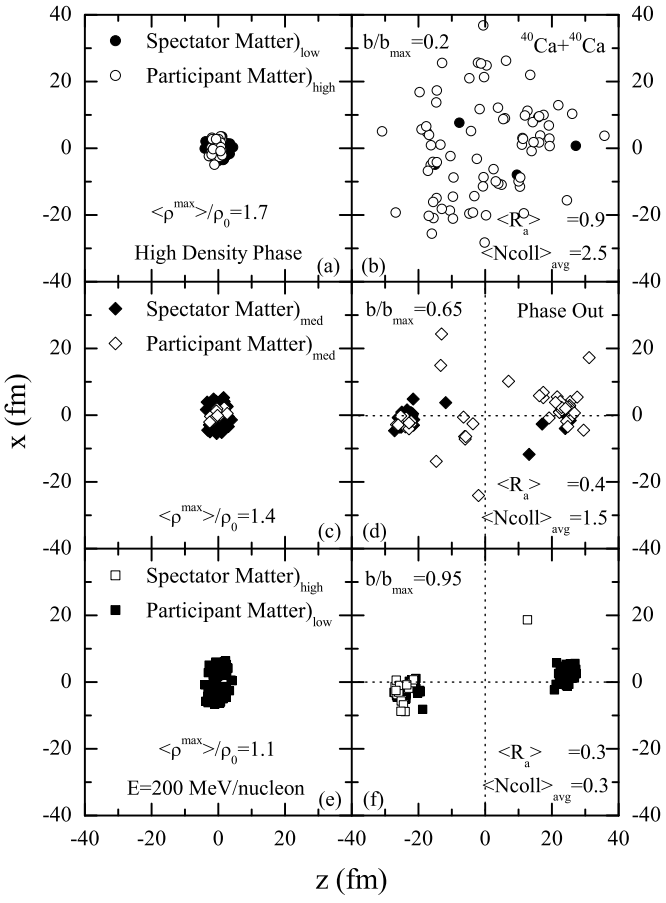

Figure 3: The time evolution of a single event of ^{40}Ca+^{40}Ca reaction at 200 MeV/nucleon. We use different impact parameters $b/b_{max} = 0.2$ (upper panel), 0.65 (middle panel), and 0.95 (bottom panel). The solid (open) symbols, again, represent the spectator (participant) matter. The high, low, and med subscripts on the spectator/participant represent the intensity of the matter, being high, low or medium for a particular reaction. The displayed quantities like $< \rho^{max} > /\rho_0$, $< Ncoll >_{avg}$, and $<R_a>$ (defined in Eq. (4)) are averaged over hundreds of events.

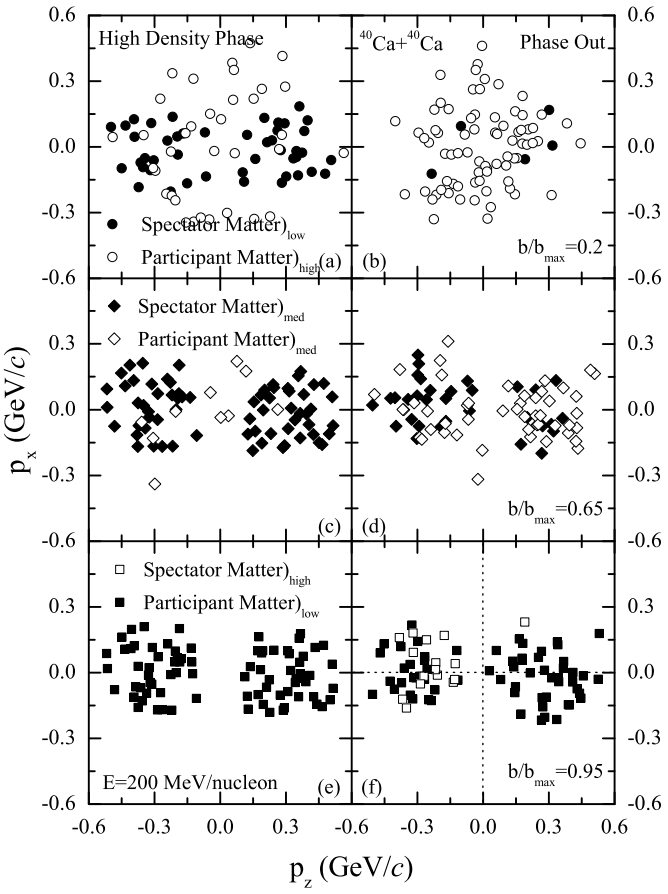

Figure 4: Same as Fig. 3, but in momentum space.

driven by the nucleon-nucleon binary collisions. The mutual two and three-body interactions dominate the physics at peripheral collision. Interestingly, though, the high density phase is nearly the same at $b/b_{max} = 0.2$ and 0.65, the final stage evolutions is quite different. In the formal one, it is more of complete disassembly whereas it is a fire-ball picture in the later case. This demonstration also points toward a very important clue for multifragmentation of these nuclei. Almost complete participant matter in central collisions does not allow any initial memory and correlations to survive. Whereas a

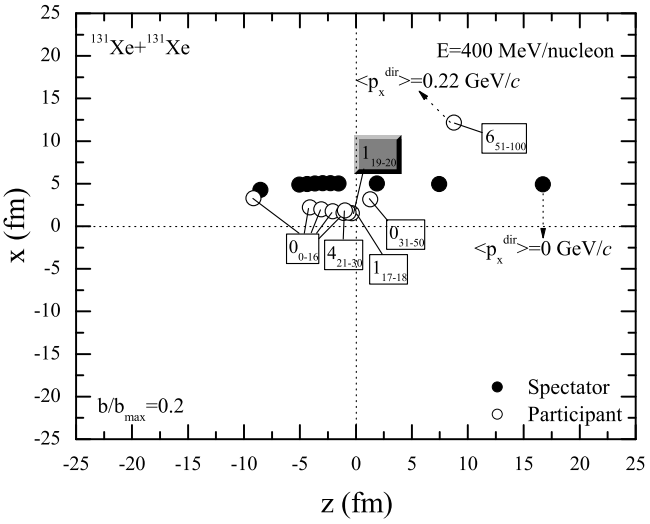

Figure 5: The trajectory of a single spectator nucleon and participant nucleon for the collision of ^{131}Xe+^{131}Xe at incident energy of 400 MeV/nucleon. The quantities in the boxes have superscripts and subscripts, representing, respectively, the number of collisions and time interval of these collisions. The shaded box is the interval for maximal density.

complete spectator matter at the peripheral geometries preserves the initial correlations. Therefore, in both these situations, one should not expect intermediate mass fragments ($5 \leq A \leq 65$) to be emitted. The formation of the intermediate mass fragments needs both the participant and spectator matter in a mild quantity. The semicentral collisions are, therefore, prefect for the study of emission of intermediate mass fragments. This has also been reported as rise and fall of intermediate mass fragments in several experimental and theoretical studies.[13, 14] Similar rise and fall also occurs with the change in the incident energies of the projectile.[12] Interestingly, baring the central collisions, no equilibrium is seen at semicental and peripheral geometries. Further from the Fig. 4, it is also evident that no substantial changes occur after the maximal high density in semicentral and peripheral collisions. However a nearly complete equilibrium can be seen in central collisions.

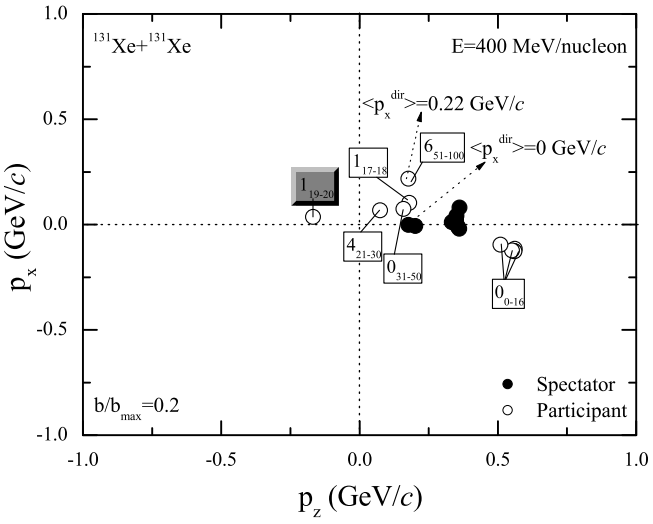

Figure 6: Same as Fig. 5, but in momentum space.

Let us now look for the changes in the phase-space with reference to the nucleon-nucleon collisions. In Figs. 5 and 6, we display the coordinate and momentum space, respectively, for a single spectator nucleon (denoted by the solid circle) and participant nucleon (denoted by the open circle). The participant nucleon has suffered a large number of binary collisions. The numeric values in the boxes represent the number of collisions faced by a nucleon. The subscripts to these values denote the time interval (in fm/c) during which these collisions happened. From Fig. 5, one notices that the trajectory of spectator nucleon remains unchanged during the entire duration of the collision. The participant nucleon, however, shifts in the transverse direction after suffering frequent collisions. Similarly, from Fig. 6, momentum space of the spectator nucleon remains unchanged. Whereas in case of participant nucleon, z-component of the velocity decreases and x-component of the velocity increases. The interesting case is the velocity profile between 19-20 fm/c. Here, velocity is negative, leading to the reversed z-coordinate between this interval. This time also happens to be the time for the maximal density. We see that the participant matter generates also

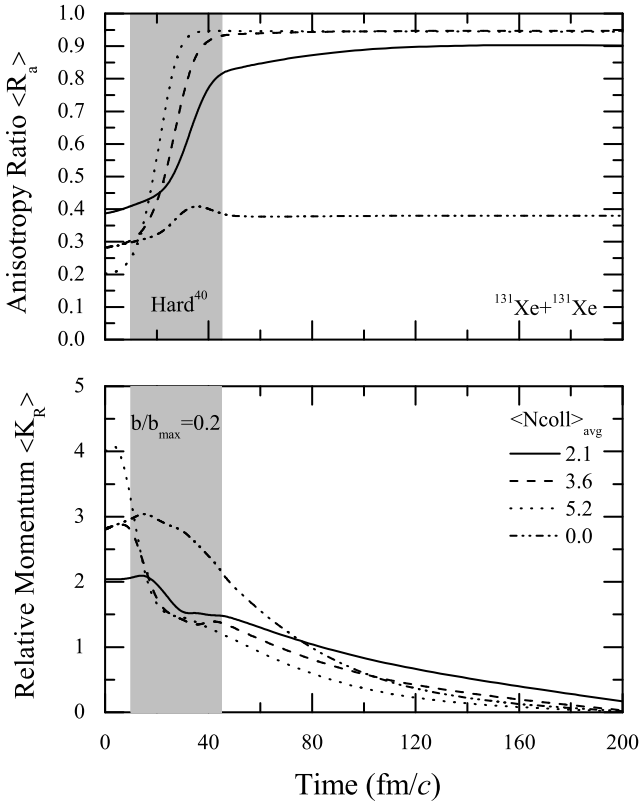

Figure 7: The anisotropy ratio $<R_a>$ and relative momentum $<K_R>$ for the case of ^{131}Xe+^{131}Xe at $b/b_{max} = 0.2$. Here different lines represent the matter having different average collisions at different incident energies. The shaded area represents the time of high density $> \rho_0$ for different reactions displayed here.

the positive transverse momentum.

In Fig. 7, we display the time evolution of anisotropy ratio $<R_a>$ and relative momentum $<K_R>$ for different average collisions experienced in a

reaction. The $<R_a>$ ratio is defined as

$$< R_a >= \frac{\sqrt{p_x^2} + \sqrt{p_y^2}}{2\sqrt{p_z^2}}. \tag{4}$$

This anisotropy ratio is an indicator of the global equilibrium of the system. This represents the equilibrium of the whole system and does not depend on the local positions. The full global equilibrium averaged over large number of events will correspond to $<R_a> = 1$. The second quantity, namely the relative momentum $<K_R>$ of two colliding Fermi spheres, is defined as

$$< K_R >=< |\vec{P}_P(\vec{r},t) - \vec{P}_T(\vec{r},t)|/\hbar >, \tag{5}$$

where

$$\vec{P}_i(\vec{r},t) = \frac{\sum_{j=1}^{A} \vec{P}_j(t)\rho_j(\vec{r},t)}{\rho_j(\vec{r},t)} \qquad i = 1, 2. \tag{6}$$

Here $\vec{P}_j$ and ρ_j are the momentum and density of the jth particle and i stands for either projectile or target. The $<K_R>$ is an indicator of the local equilibrium because it depends also on the local position r. As expected, the anisotropy ratio increases or remains almost constant whereas relative momentum decreases with increase in the number of collisions indicating better degree of global thermalization. The smaller value of ($<K_R>$) also indicates toward the better thermalization of the matter. However, once nucleon-nucleon collisions exceeds a certain limit, the thermalization does not improve with further binary collisions. Rather the nucleons prefer transparency in the system. Naturally, the higher energy projectile has a lower value of ($<R_a>$) at the start [conversely, the larger value of ($<K_R>$)]. Further, as is also evident, ($<R_a>$) ratio saturates as soon as high density phase is over. In other words, nucleon-nucleon collisions happening after high density phase do not change the momentum space significantly. One also notices that in the absence of nucleon-nucleon collisions (in Vlasov mode), almost no change is seen in $<R_a>$.

In Fig. 8, we show the normalized rapidity distribution, for a single spectator and participant nucleon. Although, the dN/dY will have the same value for both these particles, we have shifted the spectator and participant in y-axis for better clarity. Again, the values in the boxes represent the number of collisions suffered by a nucleon. The subscripts to these values represent the time interval (in fm/c). One notices that the participant nucleon, after

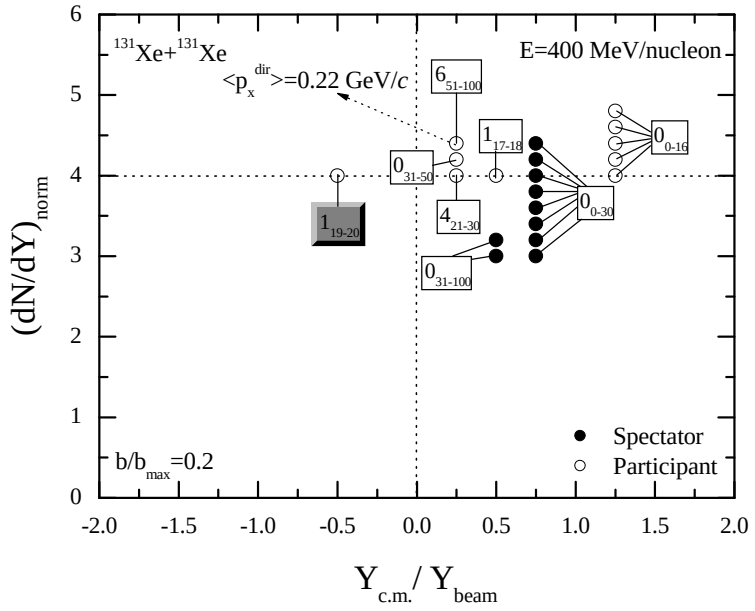

Figure 8: The normalized rapidity distribution $(\mathrm{dN/dY})_{norm}$ as a function of $\mathrm{Y}_{c.m.}/\mathrm{Y}_{beam}$. Here a single spectator nucleon and participant nucleon at different time steps is taken. The shaded box is the interval for maximal density.

suffering significant binary collisions, shifts from the projectile rapidity to midrapidity region. On the other hand, the spectator nucleon remains in the projectile rapidity region during the entire reaction.

4 Summary

We have presented the simulations of heavy-ion collisions in terms of participant-spectator matter. We find that the participant-spectator matter depends crucially on the collision dynamics and on history of the nucleon. We see that the important changes in the momentum space are due to the binary collisions experienced during the phase of high density. This otherwise was not possible with the mean field alone. The collisions push the nucleons into midrapidity region that is responsible for the formation of participant matter. This also indicates thermalization in heavy-ion collisions. Interestingly, large number of collisions, nevertheless, do not always guarantees a better degree of thermalization of the reaction.

References

[1] G. F. Bertsch and S. Das Gupta, *Phys. Rep.* **160** (1988) 189.

[2] J. Aichelin, *Phys. Rep.* **202** (1991) 233; J. Aichelin, A. Rosenhauer, G. Peilert, H. Stöcker and W. Greiner, *Phys. Rev. Lett.* **58** (1987) 1926; J. Aichelin, G. Peilert, A. Bohnet, A. Rosenhauer, H. Stöcker and W. Greiner *Phys. Rev.* **C37** (1988) 2451.

[3] H. Stöcker and W. Greiner, *Phys. Rep.* **137** (1986) 277.

[4] C. Hartnack, *Ph.D. thesis*, University of Frankfurt, Frankfurt, Germany, 1993.

[5] B. Blättel *et al.*, *Phys. Rev.* **C43** (1991) 2728.

[6] D. J. Magestro *et al.*, *Phys. Rev.* **C61** (2000) 021602(R); D. J. Magestro, W. Bauer and G. D. Westfall, *Phys. Rev.* **C62** (2000) 041603(R); G. D. Westfall *et al.*, *Phys. Rev. Lett.* **71** (1993) 1986.

[7] G. Mao, P. Papazoglou, S. Hofmann, S. Schramm, H. Stöcker and W. Greiner, *Phys. Rev.* **C59** (1999) 3381; G. Mao, L. Neise, H. Stöcker and W. Greiner *Phys. Rev.* **C59** (1999) 1674; C. Ernst, S. A. Bass, M. Belkacem, H. Stöcker and W. Greiner *Phys. Rev.* **C58** (1998) 447.

[8] R. K. Puri, P. Chattopadhyay and R. K. Gupta *Phys. Rev.* **C43** (1991) 315; R. K. Puri and R. K. Gupta *Phys. Rev.* **C45** (1992) 1837; R. K. Gupta, S. Singh, R. K. Puri and W. Scheid *Phys. Rev.* **C47** (1993) 561.

[9] C. Hartnack, R. K. Puri, J. Aichelin, J. Konopka, S. A. Bass, H. Stöcker and W. Greiner, *Eur. Phys. J* **A1** (1998) 151.

[10] A. D. Sood and R. K. Puri, *Phys. Rev.* **C70** (2004) 034611.

[11] A. D. Sood and R. K. Puri, *Phys. Rev.* **C69** (2004) 054612, and references therein.

[12] P. B. Gossiaux, R. K. Puri, C. Hartnack and J. Aichelin Nucl. Phys. **A619** (1997) 379; R. K. Puri and S. Kumar, *Phys. Rev.* **C57** (1998) 2744; J. Dhawan and R. K. Puri *Phys. Rev. C*- to be submitted.

[13] M. B. Tsang *et al.*, *Phys. Rev Lett.* **71** (1993) 1502; A. Schuttauf *et al.*, *Nucl. Phys.* **A607** (1996) 457; M. Begemann-Blaich *et al.*, *Phys. Rev.* **C48** (1993) 610; J. P. Hubbele *et al.*, *Z. Phys.* **A340** (1991) 263; N. T. B. Stone *et al.*, *Phys. Rev. Lett.* **78** (1997) 2084.

[14] G. Peilert, H. Stöcker, W. Greiner, A. Rosenhauer, A. Bohnet and J. Aichelin *Phys. Rev.* **C39** (1989) 1402; Li Zhuxia, C. Hartnack, H. Stöcker and W. Greiner, *Phys. Rev.* **C44** (1991) 824.